ACTA MONTANA IGt (1992)
Series A, No. 1(87), 89—102

DEFORMATIONAL CHARACTERISTICS AND ACOUSTIC EMISSION IN LOADED MAGNESITE SAMPLES

JAN KOZÁK[a], TOMÁŠ LOKAJÍČEK[b], VLADIMÍR RUDAJEV[a] and JAN VILHELM[a]

[a] *Institute of Geotechnics, Czechoslovak Academy of Sciences, V Holešovičkách 41, 182 09 Prague, Czechoslovakia*
[b] *Geophysical Institute, Czechoslovak Academy of Sciences, Boční II/1401, 141 31 Prague, Czechoslovakia*

Abstract: The results of deformational/acoustic measurements on magnetite samples subjected to uniaxial compression are presented. It was found that sudden changes in the deformational parameters were reflected in the changes of the frequency pattern of radiated seismoacoustic impulses. Distinct frequency changes occurred before the irreversible sample deformation; therefore, they can be regarded as the precursors of sample instability.

Key words: magnesite samples; loading; seismoacoustic emission; stress-strain curve; irreversible deformation; frequency spectra; precursors of sudden instability

1. INTRODUCTION

The stability of mining openings during chamber excavation depends mainly on the strength of the interchamber pillars. As the excavation continues, the loading of the pillars increases, especially in the vertical direction. In the first approach the above situation can be simulated under laboratory conditions by uniaxial loading of rock samples. In studying brittle fracturing of rock samples under compression, seismoacoustic (SA) effects have been investigated and utilized by numerous authors (e.g. Mogi, 1962, 1968; Scholz, 1968; Byerly and Lockner, 1971; Sondergeld and Estley, 1981; Hardy, 1972). The main aim of the work in this field is to determine the prognostical parameters, which should indicate the individual stages of sample destruction during the loading process. In the presented paper the question of the first onset frequencies of SA impulses and brittle fracture locations are discussed. The results obtained indicate that the changes in sample deformation are reflected chiefly in the amplitude-frequency spectra of the SA signals. Considerable frequency changes can be interpreted as a precursor of the overall sample rupture. The measurements were carried out under the auspices of the East-Slovakia Magnesite Mines, Lubeník.

2. EXPERIMENTAL

The magnesite samples treated were prepared from magnesite deposits in Jelšava, SE Slovakia (mild grained magnesite). They were rectangular in shape and denoted

Mag 1 and Mag 2. The square bases of the models, 100 × 100 mm, which were in contact with the press, were specially treated in order to avoid irregular loading of the model. The height of the model was 300 mm. Pairs of tensometric pick-ups (arranged crosswise) were located in the middle of all four sides of the model to record both transverse and longitudinal deformations in the course of loading the model.

Eight SA pick-ups, fixed to the model surface, were used to record radiated pulses and to localize SA foci. The samples were compressed in a WPM hydraulic press operating at loads of up to 3000 kN. The loading rate was adjusted to 5 kN/min, which corresponded to a compression increment of 5 MPa/min.

The following parameters were monitored and analysed as the function of the load:

a) sample deformation,
b) SA foci location,
c) frequencies of SA signals.

Ad a)

Both longitudinal and transverse deformations were monitored by means of a UPM-40 tensometric bridge, the data were stored in an SAPI-81 unit and, together with the load values, printed in tabular form.

The relative deformation of the loaded samples ($\Delta l/l$) was measured with an accuracy of 10%, which amounted to 300 μm for the models treated.

The patterns of the stress-strain changes for the treated models are demonstrated in Fig. 1. The linearity of Hooke's relations for longitudinal and even transverse deformations is preserved to approx. 68% of the compression strength (= stress 55 MPa) for Mag 1 and to approx. 95% of the compressive strength (= stress 55 MPa) for Mag 2, respectively. It is evident from the slopes of the stress-strain curves (Fig. 1) that the longitudinal deformation patterns deviate from a linear course. Although the square bases of the models were specially treated to avoid irregular deformation, the model was irregularly deformed during the loading, probably due to its inner heterogeneous structure.

After the above the critical stress value of 55 MPa had been attained, significant deformational changes occurred. This process was connected with irreversible changes signalling the initiation of total fracturing of the tested structure. The tensometrical analysis that allows us to conclude that the stability of both test samples was critically disturbed at a stress value of 55 MPa. Therefore the tensometrical analysis is not very suitable for prognosticating a fracture process because it already reflects the total breakdown of the loaded structure. This agrees with the fact that the critical strength (55 MPa) corresponds to different percentage values (68% and 85%) of the compressional strength for Mag 1 and Mag 2, respectively.

Ad b)

The location of SA foci was determined by means of the kinematic analysis of *P*-wave arrival times. The location of acoustic foci was based on the kinematic methods. Therefore, special ultrasonic measurements by eight pick-ups fixed to all

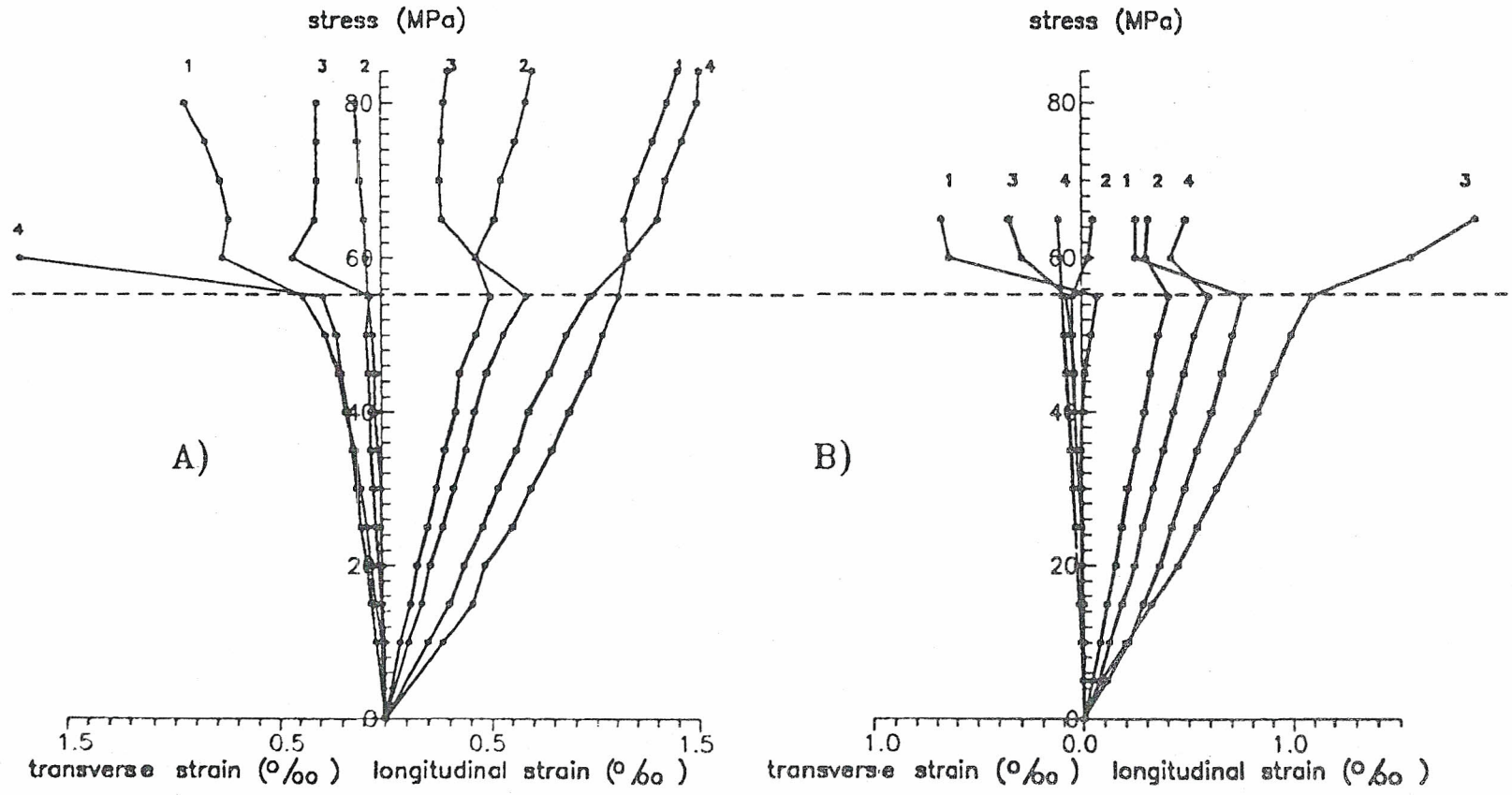

Fig. 1. A) The deformation pattern — Mag 1. Numbers 1–4 denote tensometers (cf. Fig. 2). B) The deformation pattern — Mag 2. Numbers 1–4 denote tensometers (cf. Fig. 2). The black points in the diagram denote the levels of measurements.

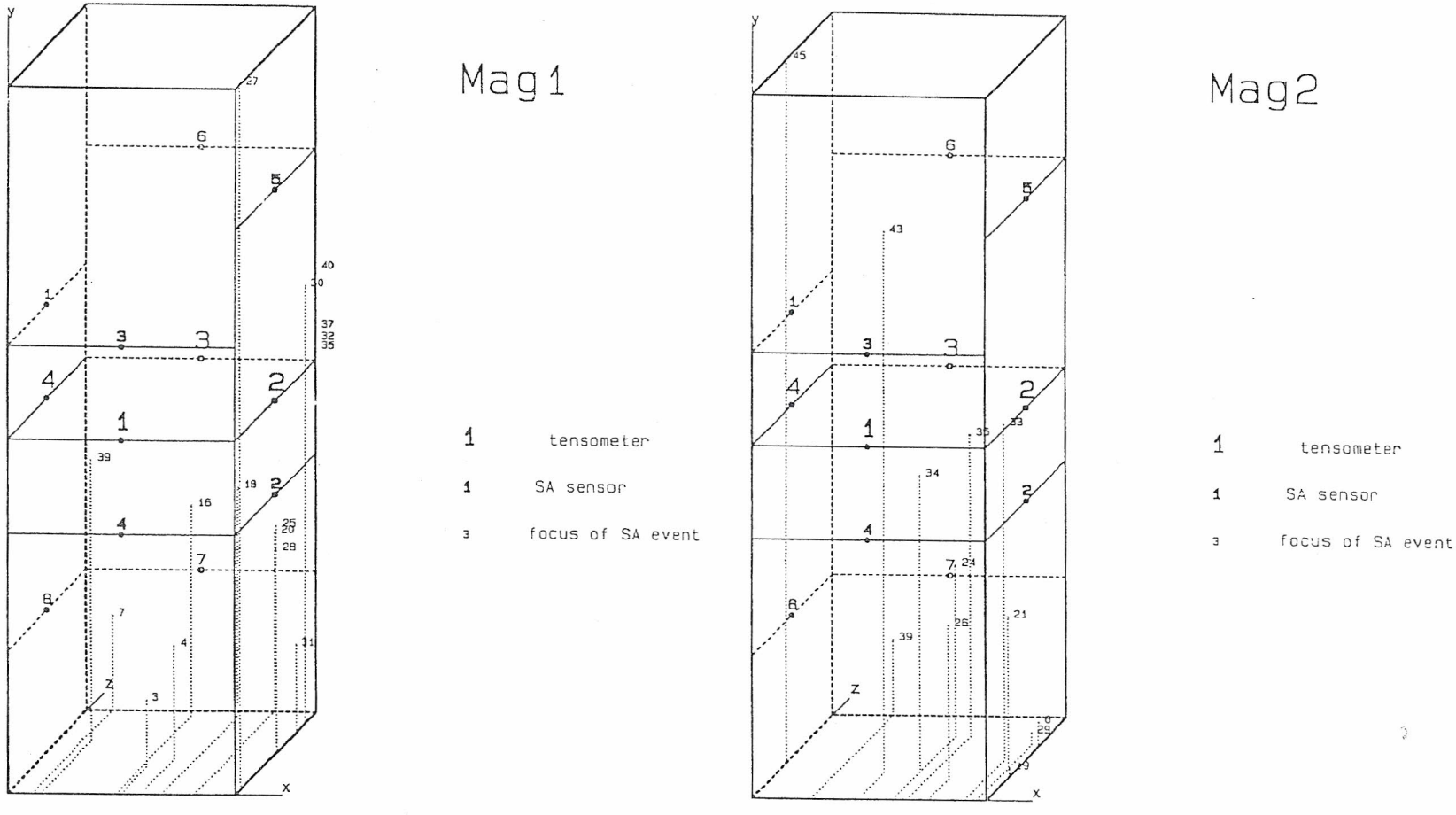

Fig. 2. Models Mag 1 and Mag 2 — positions of sensors and focus events. The size of the models — 100 × 100 × 300 mm.

four vertical model faces were performed to establish the P-wave velocity. In both the models the determined value, $v_p = 6000\ m.s^{-1}$, was then used to localize the foci kinematically.

In localizing the individual SA emission foci only those records (of the above eight pick-ups) were treated, in which the P-wave first onsets were quite distinct on the records of at least five pick-ups of eight. This condition reduced the number of treated events to 38% (for Mag 1) and to 26% (for Mag 2); the results are shown in Fig. 2. As for Mag 1, all 16 localized foci were found inside the model or on the model surface: 13 of these foci were on the lateral model walls. This can be understood as a certain surface SA focus clustering, however, also geometrical deformation of the model under load (bending) can contribute to this apparent focus cumulation.

The Mag 2 model, in which nearly 1/2 of the foci (five out of 12 ones), namely Nos. 24, 26, 33, 34 and 35, were located in one inner model zone, provides a better picture of SA foci localization; they seem to occupy the space in which the total fracture of the model could be initiated. Unfortunately, no finer tool was available to prove this. Also for the Mag 2 model all computed SA foci were found inside the model or on its surface.

The results obtained display that two types of fracturing occurred during sample loading: surface failure (probably due to sample bending) and entire crack occurrence which the mechanism of the fracturing process in nature better.

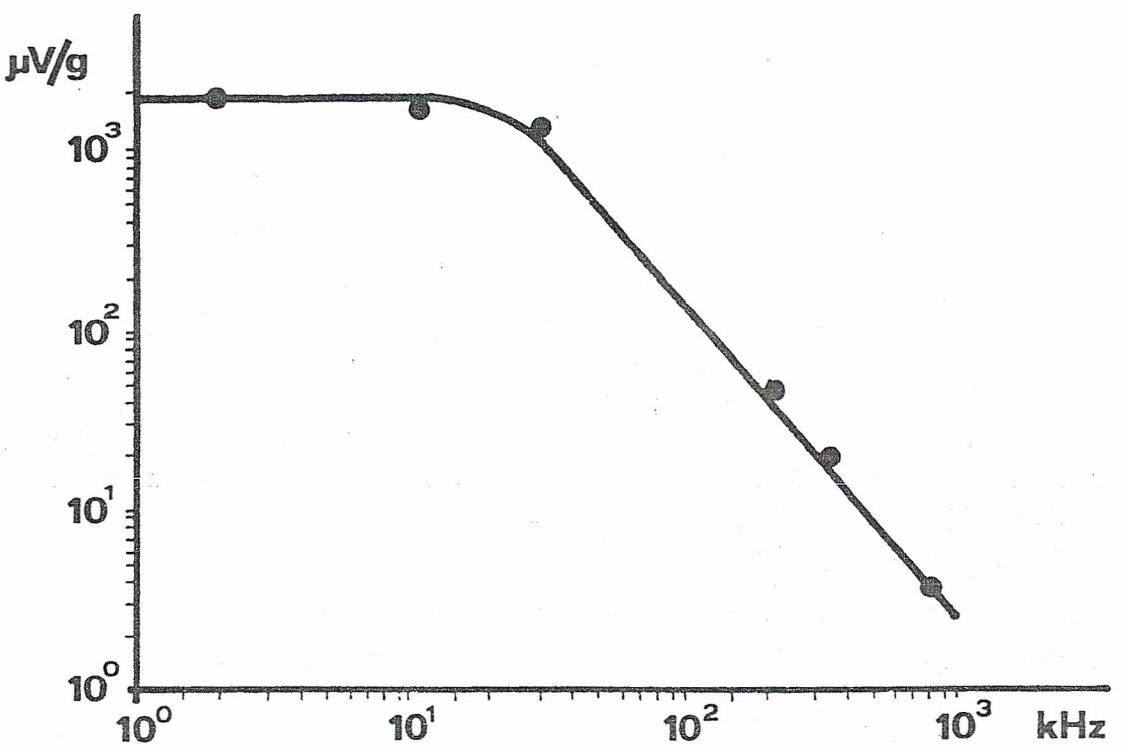

Fig. 3. Frequency response of the SA transducers used.
μV/g – microvolts per acceleration unit ($cm.s^{-2}$).

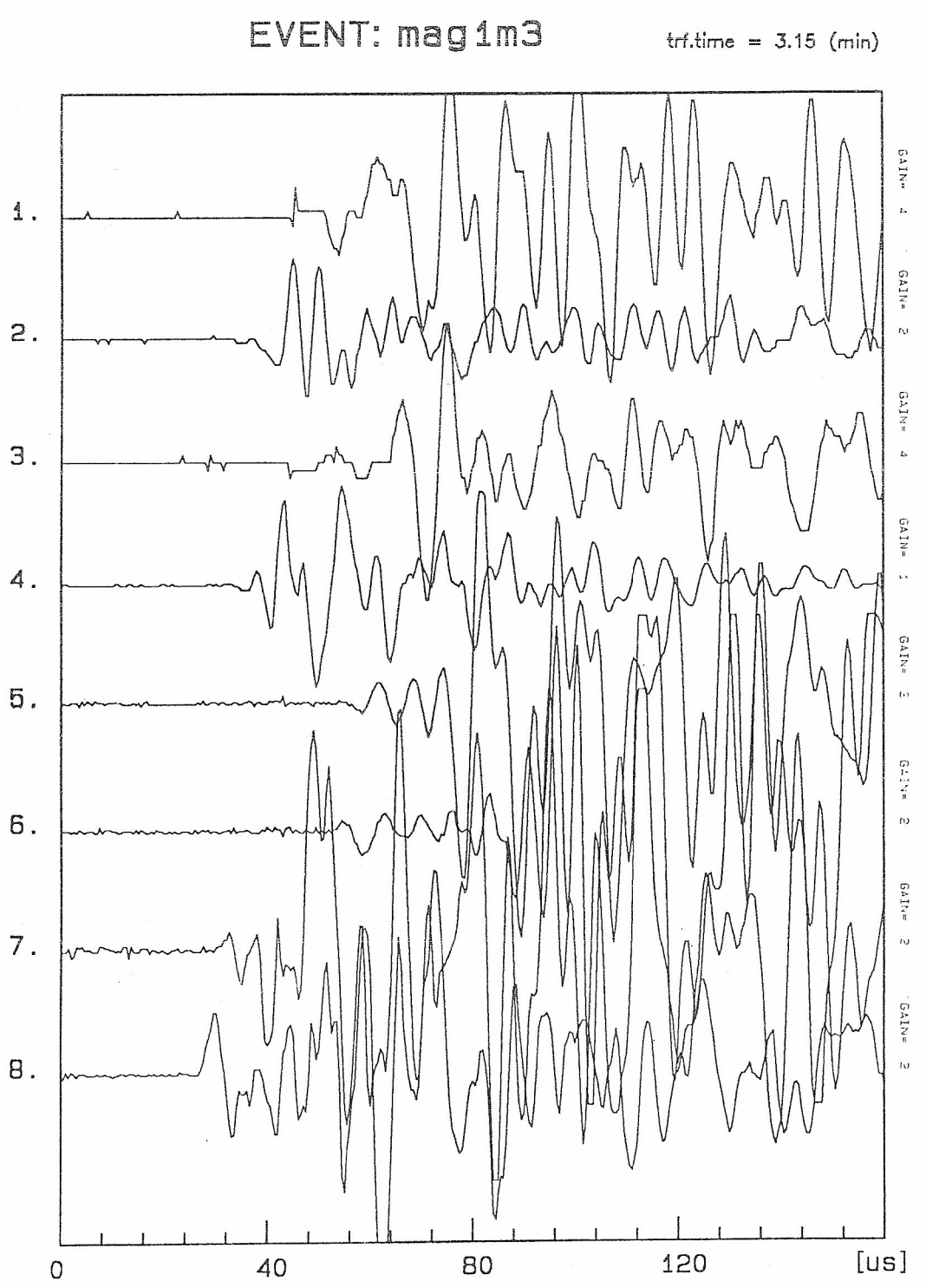

Fig. 4. A) An example of the record of SA event No. 3. Focus inside specimen Mag 1. The gain values for the individual channels are given on the right-hand vertical axis (A-values are given in μV).

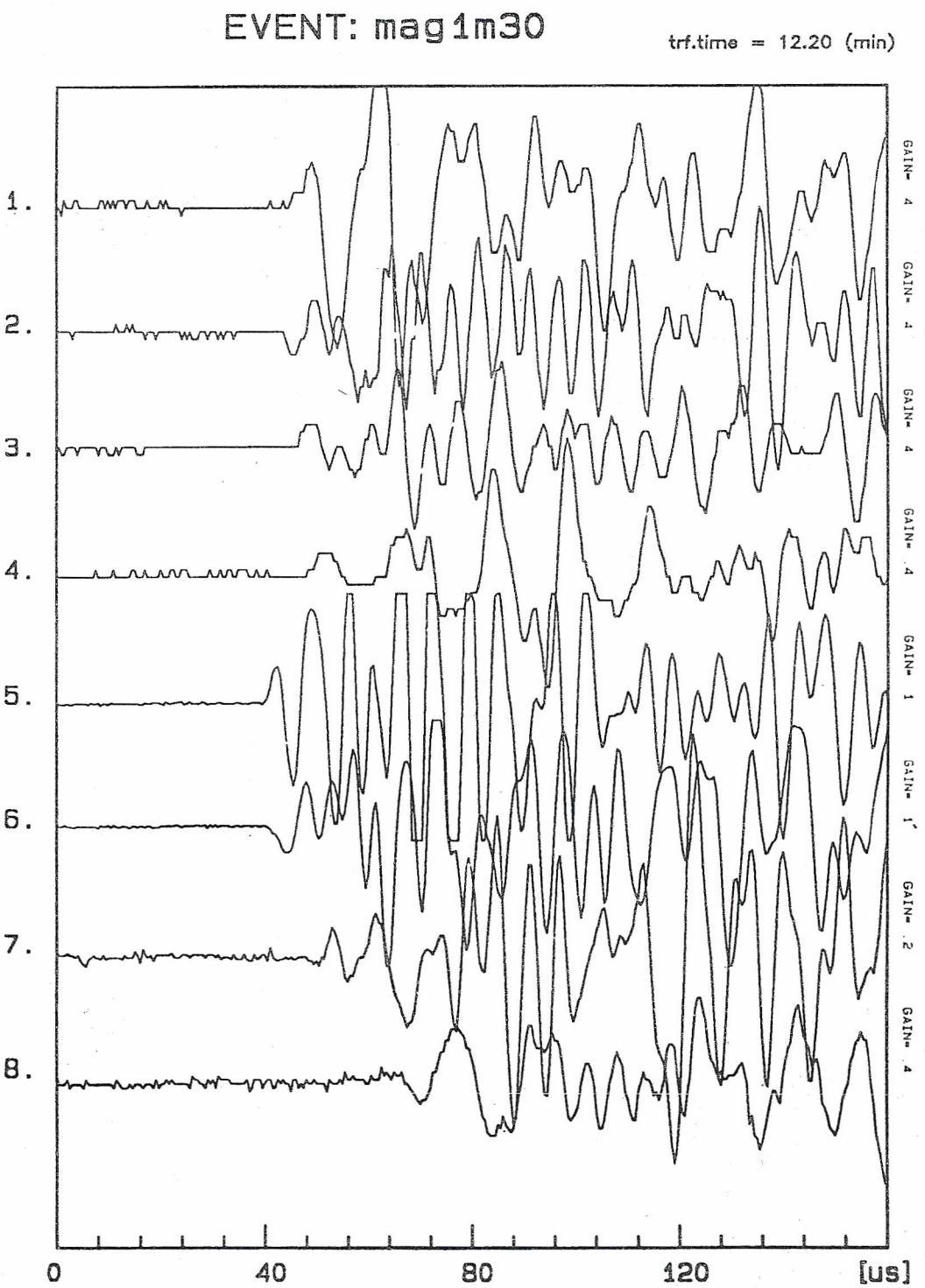

Fig. 4. B) An example of the record of SA event No. 30.
Focus near the surface. For the gain, see A).

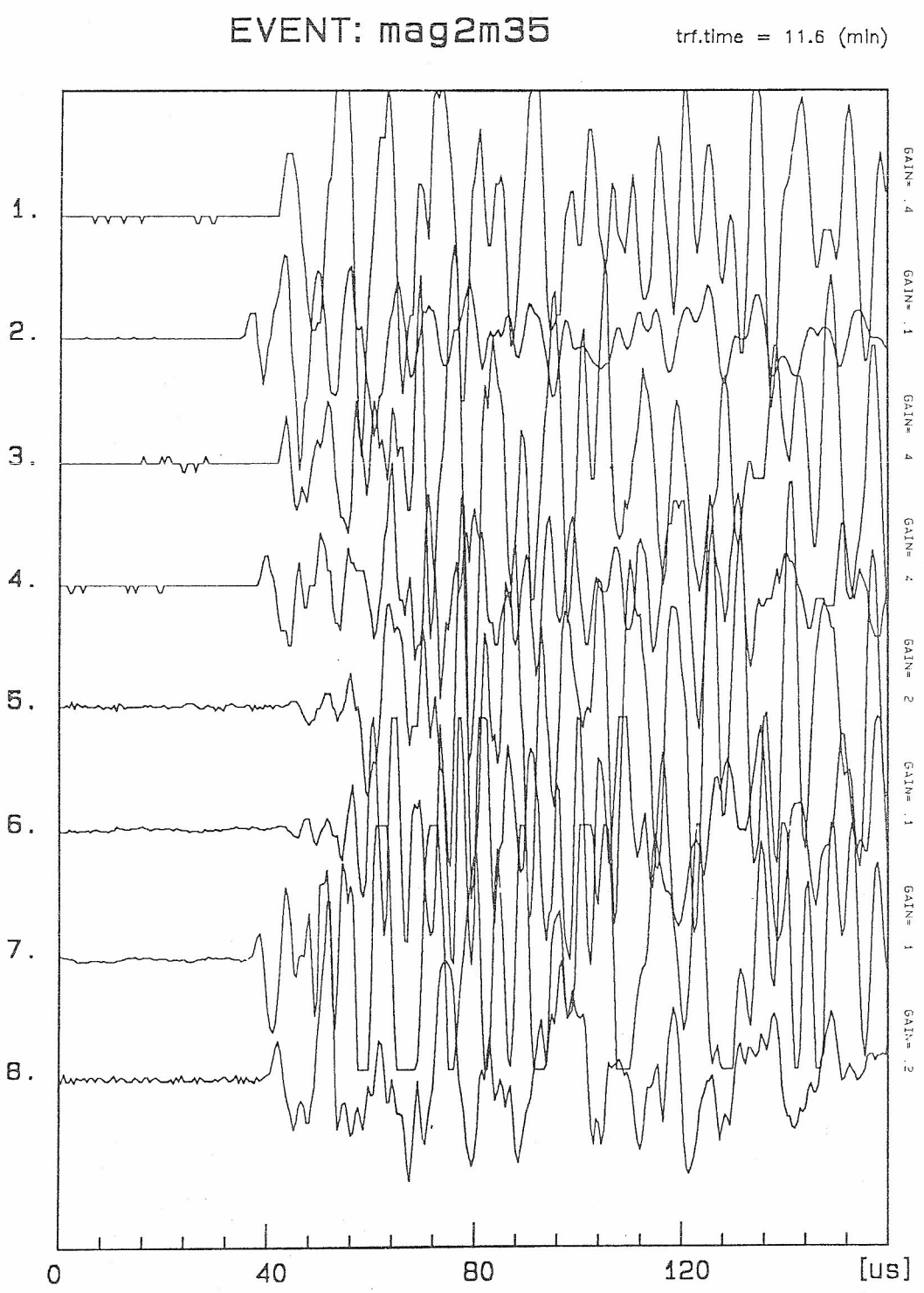

Fig. 5. A) An example of the record of SA event No. 35. Focus inside specimen Mag 1. For the gain, see Fig. 4, A).

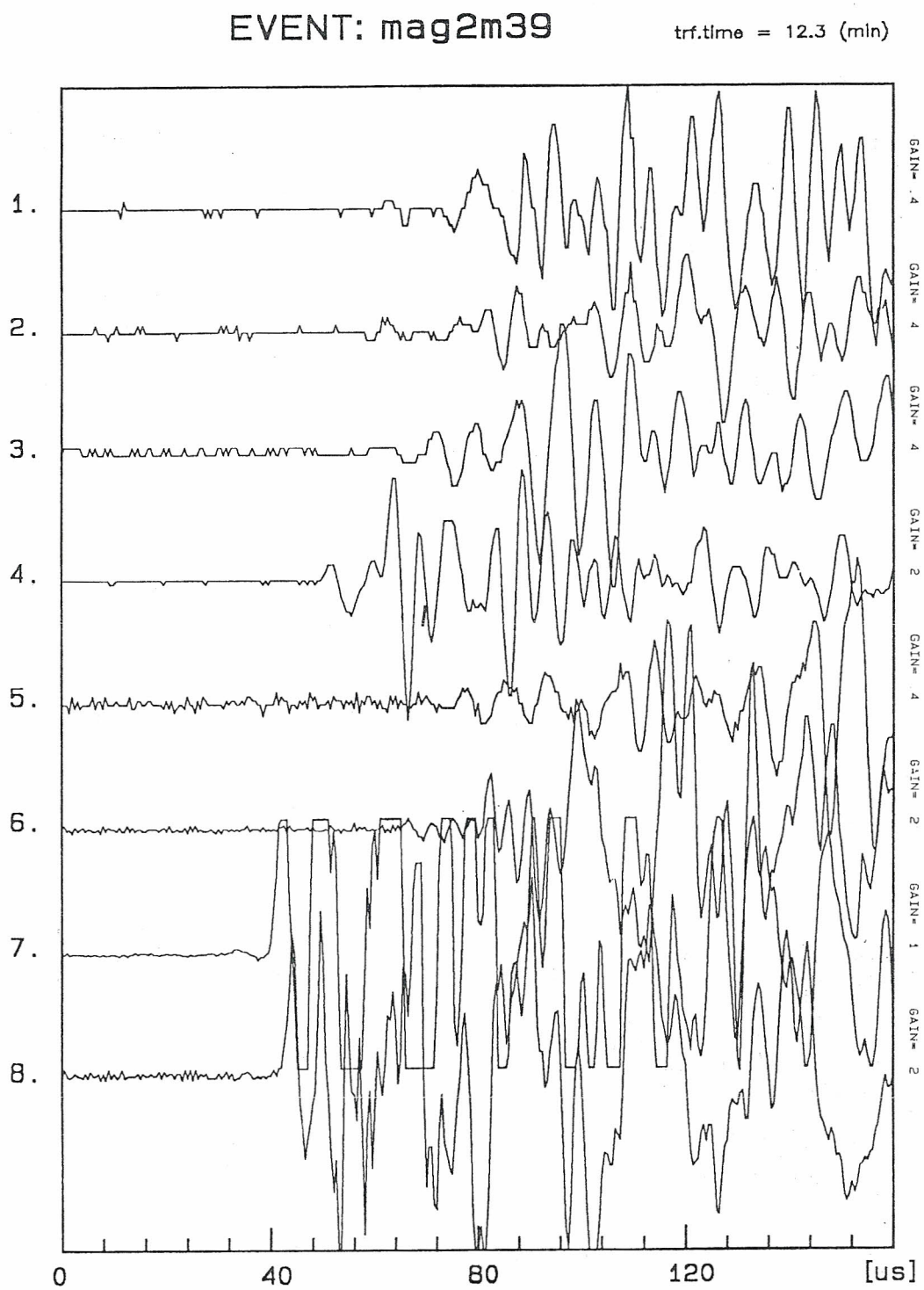

Fig. 5. B) An example of the record of SA event No. 39. Focus near the surface of specimen Mag 2. For the gain, see Fig. 4, A).

Ad c)

SA signals were recorded by cylindrical (diameter 12 mm) ultrasonic TL-86 accelerometers operating with constant sensitivity in the frequency range up to 100 kHz. The recording band extended to 1 MHz (see Fig. 3). Radiated signals were stored in four Datalab 912 double-channel transient recorders. The sampling frequency was set to 2 MHz. The set-up operated in the waiting mode; the monitored digital data were then stored on an additional memory disc. 9.6 s were needed to

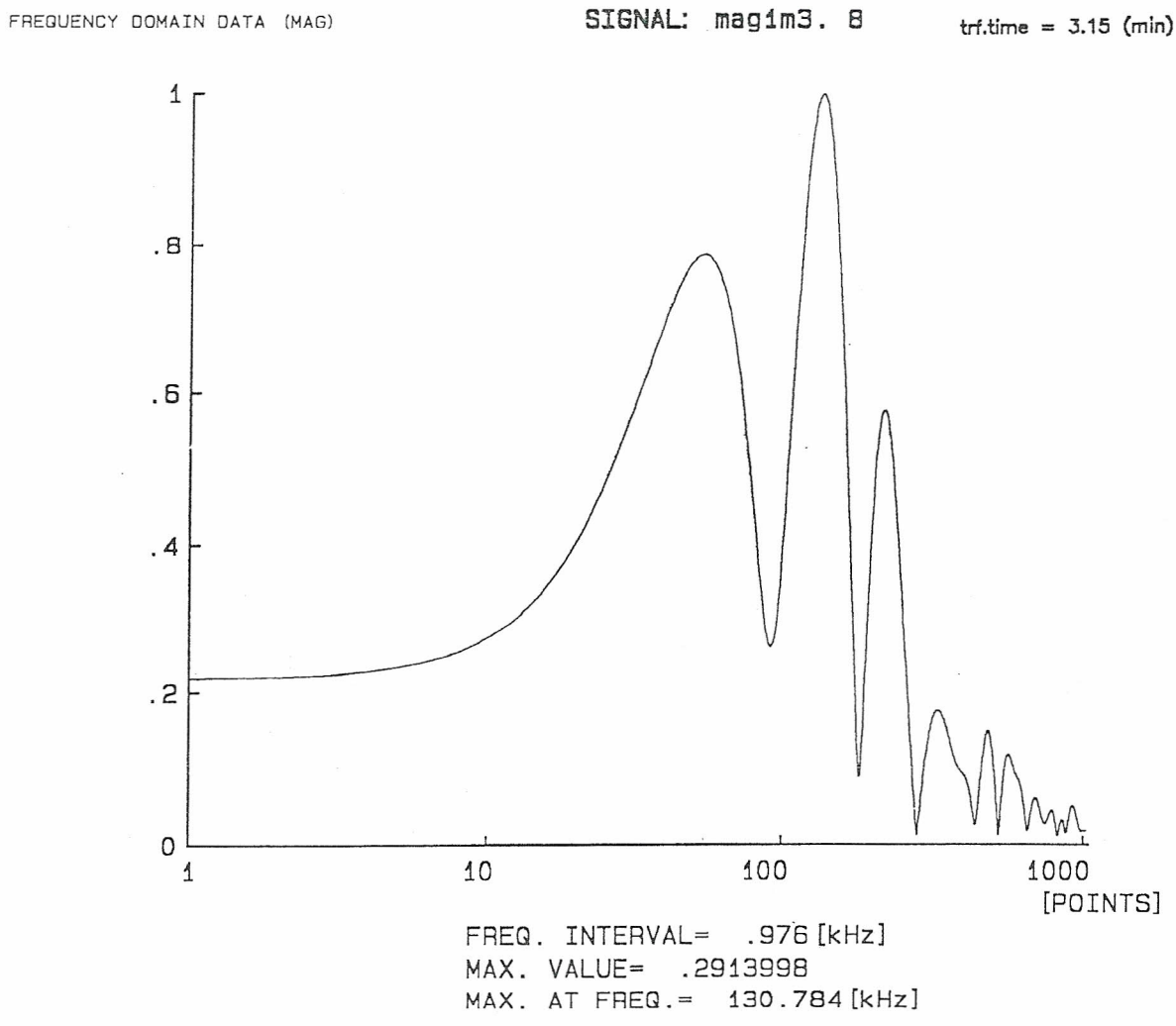

Fig. 6. Spectrum of the pulse recorded by the 8th channel, specimen Mag 1, event No. 3.

record and store one SA event in the eight-channel system used; during this time the system was out of operation.

In the course of loading up to total destruction of the samples, 42 pulses (Mag 1) and 46 pulses (Mag 2) were recorded. The number of SA pulses increased with increasing load. After reaching the stress value, equal to approx. 60% of the

maximum strength, the time gap between the occurrence of the individual pulses dropped below 10 s, which caused that some SA pulses were not recorded.

The average time duration of the SA pulses was about 1–2 ms. Owing to the sample size and to velocity $v_p = 6000\ \mathrm{m.s^{-1}}$, the time of non-interferential signals was less than 20 μs depending on the configuration of the face and the acoustic pick-ups; this time corresponded to the period of one wavelength relative to the prevailing pulse frequency up to 100 kHz.

The examples of the records of SA impulses for samples Mag 1 and Mag 2 are given in Figs. 4 A), B) and 5 A), B). The occurrence in time of the events in Figs. 4 and 5 can be found on the time axis of Fig. 7 B) according to the transfer time values given in the right upper corners of Figs. 4 and 5.

Changes in the prevailing frequencies of the emitted pulses were observed during the deformational and structural changes, which took place in the tested samples under load. Wave patterns subjected to the frequency analysis were selected so that they covered the whole process of the sample deformation.

The wave patterns recorded by pick-up No. 8 were frequency analyzed. For example, see Fig. 6. In the preliminarily recorded spectrum patterns several maxima, related to different interference groups, were clearly expressed. They can be derived mainly from the geometry of the model, focus parameters and local properties of the model medium. To minimize the effects of the geometry of the model (and its manifestations in the obtained spectra), only the first wave onsets (10 μs) corresponding approx. to one wavelength were subjected to the final frequency evaluation. By comparing the spectrum patterns with the appropriate wave recordings by visual type analysis, we selected the representative maximum in the spectra. It was observed that the selected spectrum maxima had constant values while the model was being loaded up to a certain value. Further loading of the model results in a rapid shift of the frequency maxima to higher frequencies. This shift obviously corresponded to the size of the fractured elements participating in the signal radiation.

Up to 62% of the sample strength these frequencies ranged from 140–160 kHz for both models, Mag 1 and Mag 2. From this point a rapid growth of the pulse frequencies was observed, which culminated at 180 kHz and 200 kHz (= 68% for Mag 1 and 88% for Mag 2 of the sample strength, respectively) (see Fig. 7). The last loading interval is characterized by a sharp decrease of the first onset frequencies, approximately to 90–125 kHz.

On the basis of the comparison of the observed deformational patterns and frequency changes, one can conclude that the initial frequency changes are not reflected in the deformation patterns. From this viewpoint, their frequency changes seem to be promising in signalling the beginning of the total destruction of the sample (see the lower dashed line in Fig. 7). The maximum value of the frequencies displays a clear response to the deformation pattern and reflects significant changes in the sample structure. These results indicate that even though the stress values had not yet reached their maxima, a rapid frequency shift to higher values could be regarded as a precursor in the process of sample failure. From this point on,

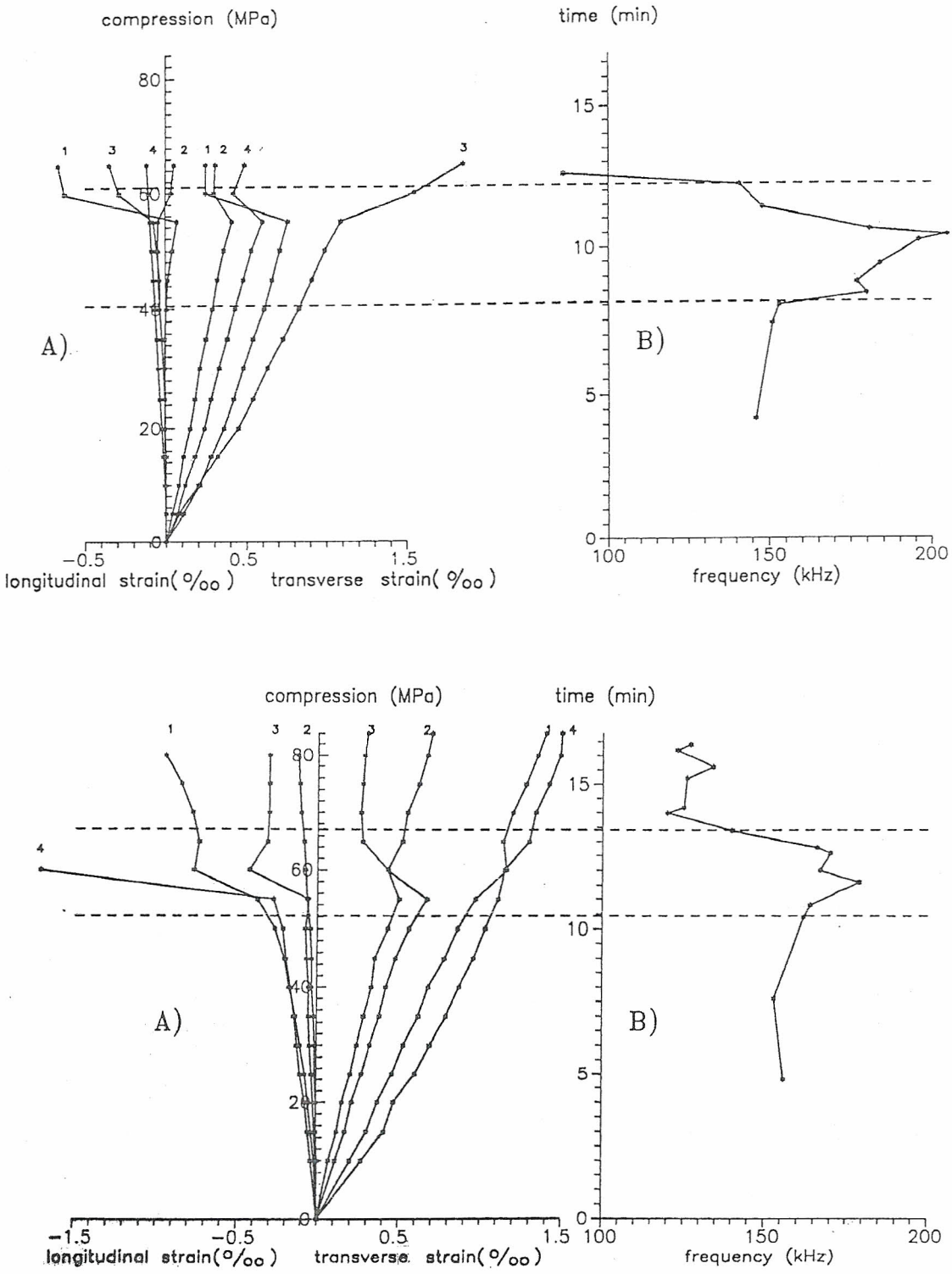

Fig. 7. Stress-strain curves (A), and frequencies of SA events (B). Top – Mag 1, bottom – Mag 2. The dots in both the B-diagrams denote the first onset frequencies of treated pulses.

the danger of a large-scale destructive process can be expected. Also splitting the model into large section, corresponding to the frequency decrease observed in the last interval of loading, is in good agreement with the above interpretation.

It should be noted that the presented results do not seem to depend on the sample size; similar relations betweeen deformational and SA parameters as presented here were also observed in smaller samples under load (5 × 5 × 10 cm) (see Kozák *et al.*, 1988).

3. CONCLUSIONS

The results presented above reflect the specific behaviour of the frequency of the treated SA pulses as related to the deformational parameters of the investigated samples under load. It was found, by comparing the stress-strain diagram and the SA emission pattern, that the growth of the first onset frequencies occurred prior to pronounced sample deformation, i.e., these frequencies originated at the stage of loading at which the tensometric data displayed no rapid deformation changes. The considerable period changes, observed for the first onsets of the acoustic pulses in question, have been interpreted, in first approximation, as a possible precursor of the sudden failure of the loaded sample. For a given set-up, however, one should bear in mind that the frequency changes of radiated pulses can also be partially affected by the sample structure and size, by the rate of loading and especially by focus locations of SA pick-ups. Therefore, an unambiguous verification of the prognostic character of the above frequency changes in the course of loading would require more extensive experimental evidence.

ACKNOWLEDGEMENTS

The authors are indebted to Dr. J. Vaněk of the GFI CSAS, Prague, for stimulating comments and recommendations, and to Dr. Z. Potužák of the IGt CSAS, Prague, for his assistance during the experiment.

REFERENCES

Byerlee, J.D. and D. Lockner (1977). Acoustic emission during fluid injection into rock, in *Proceedings of the 1st Conference on Acoustic Emission/Microseismic Activity in Geologic Structures and Materials*, edited by H.R. Hardy and F.W. Leighton, *Trans. Tech. Publications*, Clausthal, Germany, 87–98.

Hardy, H.R. (1972). Application of acoustic emission techniques to rock mechanics research, *ASTM Spec. Tech. Publ. STP* 505, 41–83.

Kozák, J., T. Lokajíček, Z. Potužák, and V. Rudajev (1988). Testing magnesite samples from the Lubeník locality, Res. Rept., Geophysical Institute, CSAS, Prague (in Czech).

Mogi, K. (1962). Magnitude-frequency relation for elastic shocks accompanying fractures of

various materials and some related problems in earthquakes, *2nd Bull. Earthquake Res. Inst.*, Tokyo Univ. **10**, 831–853.

Mogi, K. (1968). Source locations of elastic shocks in the fracturing process in rocks, *1st Bull. Earthquake Res. Inst.*, Tokyo Univ. **46**, 1103–1125.

Scholz, C.H. (1968). Experimental study of the fracturing process in brittle rock, *J. Geophys. Res.* **73**, 1447–1453.

Sondergeld, C.H. and I.H. Estley (1981). Acoustic emission study of microfracturing during the cyclic loading of Westerly granite, *J. Geophys. Res.* **86**, 2915–2924.

DEFORMAČNÍ CHARAKTERISTIKA A AKUSTICKÁ EMISE NA ZATĚŽOVANÝCH VZORCÍCH MAGNEZITU

Jan Kozák, Tomáš Lokajíček, Vladimír Rudajev a Jan Vilhelm

Jsou uvedeny výsledky deformačních a akustických měření na vzorcích magnezitu, které byly jednoose zatěžovány. Bylo zjištěno, že náhlé změny průběhu deformací se projevují i ve změnách frekvenčního obsahu vyzářených akustických pulsů. Zřetelné frekvenční změny impulsů byly pozorovány již před nevratnými deformacemi, takže mohou být považovány za předzvěsti nestability vzorků.

Received 19 August 1991